Stem Cells Translational Medicine, 2025, **14**, szaf013
https://doi.org/10.1093/stcltm/szaf013
Advance access publication 15 May 2025
Original Research

Zinc finger protein 750 is a novel regulator of osteoblast differentiation and bone homeostasis by transcriptionally deactivating SNAI1 signaling

Xiaoli Shi[1,2,3,‡], Xueli Jia[1,‡], Wei Liu[1], Liwen Shi[1], Zheng Yang[2], Jie Zhou[1], Xiaoxia Li[*,2], Baoli Wang[*,1]

[1]NHC Key Lab of Hormones and Development and Tianjin Key Lab of Metabolic Diseases, Tianjin Medical University Chu Hsien-I Memorial Hospital & Institute of Endocrinology, Tianjin 300134, People's Republic of China,
[2]College of Basic Medical Sciences, Tianjin Medical University, Tianjin 300134, People's Republic of China,
[3]Present address of Xiaoli Shi: Department of Laboratory, Jincheng People's Hospital, Jincheng, Shanxi 048000, People's Republic of China

[*]**Corresponding authors.** Baoli Wang, NHC Key Lab of Hormones and Development and Tianjin Key Lab of Metabolic Diseases, Tianjin Medical University Chu Hsien-I Memorial Hospital & Institute of Endocrinology Huan-Rui-Bei Road, Tianjin 300134, People's Republic of China. E-mail: blwang@tmu.edu.cn; Xiaoxia Li, NHC Key Lab of Hormones and Development and Tianjin Key Lab of Metabolic Diseases, Tianjin Medical University Chu Hsien-I Memorial Hospital & Institute of Endocrinology Huan-Rui-Bei Road, Tianjin 300134, People's Republic of ChinaE-mail: Lixx@tmu.edu.cn
[‡]The authors contributed equally to the work.

Abstract

Zinc finger protein 750 (ZNF750) has been identified as a potential tumor suppressor across multiple malignancies. Nevertheless, the specific involvement of ZNF750 in the regulation of mesenchymal cell differentiation and bone homeostasis has yet to be elucidated. In the current study, we observed a substantial presence of ZNF750 in bone tissue and noted alterations in its expression during osteogenic differentiation of mesenchymal progenitor cells. Functional experiments indicated that ZNF750 promoted osteogenic differentiation while impeding adipogenic differentiation from mesenchymal stem/progenitor cells. Further mechanistic investigations revealed that ZNF750 transcriptionally suppressed the expression of Snail family transcriptional repressor 1 (SNAI1) by binding to the proximal promoter region of Snai1 gene, thereby activating Wnt/β-catenin signaling. SNAI1 exerted opposing effects on cell differentiation towards osteoblasts and adipocytes in comparison to ZNF750. The overexpression of SNAI1 counteracted the dysregulated osteogenic and adipogenic differentiation induced by ZNF750. Furthermore, the transplantation of Znf750-silenced bone marrow stromal cells into the marrow of wild-type mice resulted in a reduction in cancellous and cortical bone mass, alongside a decrease in osteoblasts and an increase in marrow adipocytes, while the number of osteoclasts remained unchanged. This study presents the first demonstration that ZNF750 regulates the differentiation of osteoblasts and adipocytes from mesenchymal stem/progenitor cells by transcriptionally deactivating SNAI1 signaling, thereby contributing to the maintenance of bone homeostasis. It suggests that ZNF750 may represent a promising therapeutic target for metabolic bone disorders such as osteoporosis.

Key words: adipocyte; bone homeostasis; differentiation; osteoblast; Snail family transcriptional repressor 1; Zinc finger protein 750.

Received: 5 December 2024; Accepted: 2 April 2025.

Graphical Abstract

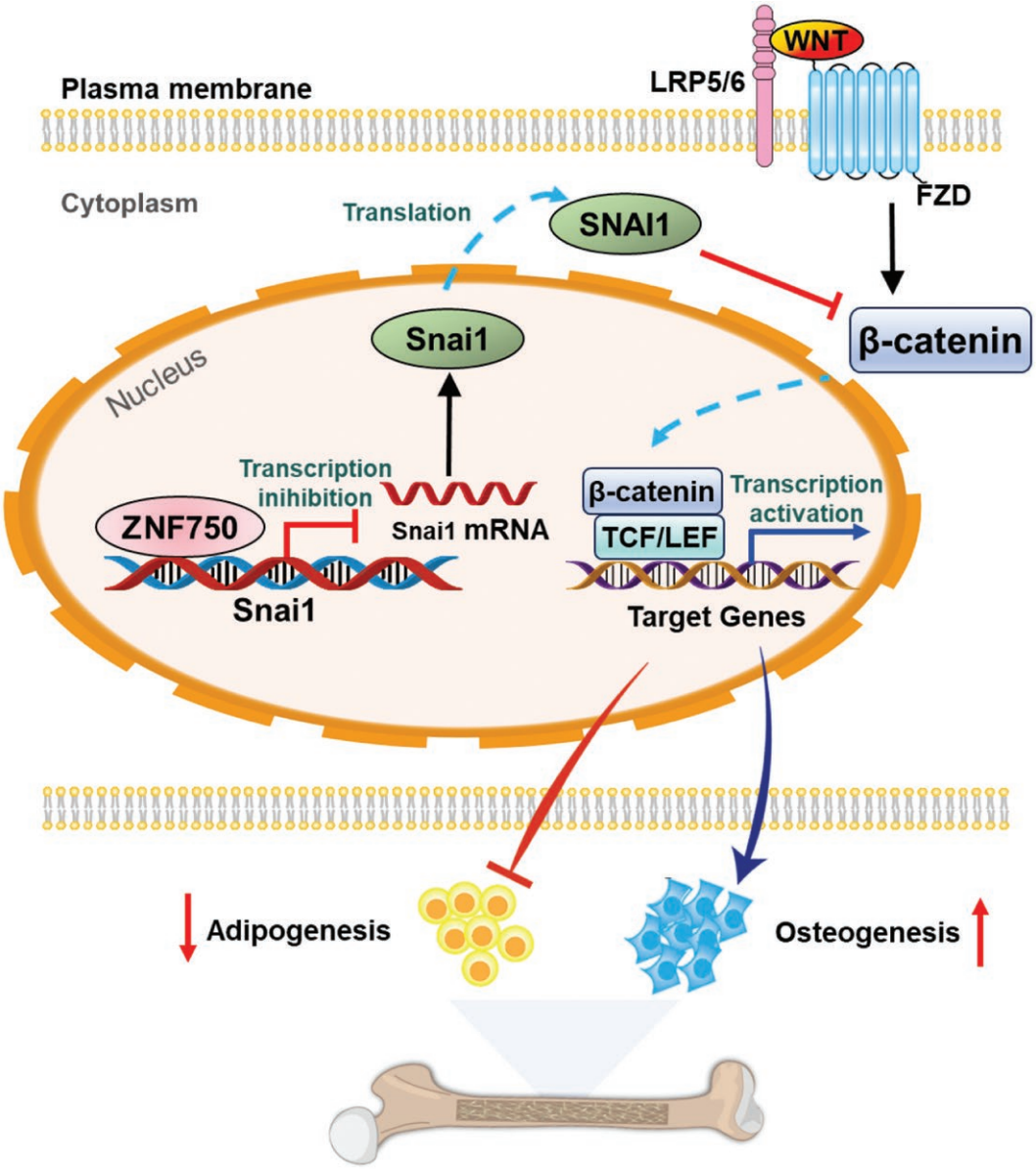

SNAI1 protein serves to inactivate Wnt/β-catenin signaling in mesenchymal progenitor cells. ZNF750 binds to the promoter of Snai1 and downregulates Snai1 expression, thereby activating Wnt/β-catenin pathway. This mechanism enables ZNF750 to facilitate osteogenic differentiation of mesenchymal progenitor cells while inhibiting adipogenesis. As a result, the expression of ZNF750 in mesenchymal progenitor cells tends to positively modulate bone mass.

Significance statement

We report that ZNF750, a zinc finger transcription factor, in mesenchymal stem/progenitor cells facilitates osteoblast differentiation and conversely inhibits adipocyte formation. The transplantation of Znf750-silenced bone marrow stromal cells into the marrow of wild-type mice resulted in a reduction in cancellous and cortical bone mass by decreasing osteoblasts and increasing adipocytes. The role of ZNF750 in osteoblast and adipocyte differentiation is associated with its transcriptional inactivation of SNAI1 expression by binding to the proximal promoter region of Snai1 gene, thereby activating Wnt/β-catenin signaling. ZNF750 may represent a promising therapeutic target for osteoporosis.

Introduction

Osteoporosis, a prevalent degenerative bone disorder among the elderly, is characterized by increased bone fragility and decreased strength, making bones more susceptible to fractures.[1] Recently, there has been a growing focus on reestablishing the balance between osteoblast-mediated bone formation and osteoclast-mediated bone resorption in osteoporosis.

Bone marrow stromal cells (BMSCs) serve as the primary origins of osteoblasts, and investigating their directed

differentiation holds promise for developing novel therapeutic approaches for osteoporosis.[2-4] Under physiological conditions, BMSCs possess comparable abilities to differentiate into both osteoblasts and adipocytes.[5-7] The recent utilization of single-cell transcriptomics has enabled the identification of distinct mesenchymal cell subpopulations, encompassing osteogenic and adipogenic subsets.[8,9] The processes of osteogenic and adipogenic differentiation are governed by a complex interplay of various transcription factors and signaling pathways. Notable signaling molecules implicated in this regulatory framework include bone morphogenetic proteins (BMPs), runt related transcription factor-2 (Runx2), osterix (OSX), the canonical Wnt signaling pathway, peroxisome proliferator-activated receptor γ (PPARγ), and CCAAT enhancer binding proteins (C/EBPs).[10-14]

Zinc finger protein 750 (ZNF750) is a transcription factor that possesses a C2H2 zinc finger motif and a nuclear localization domain. One of the extensively studied functions of ZNF750 is its involvement in the regulation of epidermal homeostasis.[15-18] In humans, mutations in this gene have been linked to seborrhea-like dermatitis with psoriasiform characteristics.[16] In mice, the genetic deletion of Znf750 has been demonstrated to compromise epidermal barrier function, attributed to diminished ceramide levels.[17] Additionally, ZNF750 has been proposed as a potential tumor suppressor in a variety of malignancies, including nasopharyngeal carcinoma,[19] oral and esophageal squamous cell carcinomas,[20,21] and breast cancer,[22] etc.

To date, the role of ZNF750 in the regulation of mesenchymal cell differentiation and bone homeostasis remains unknown. In this study, we present evidence indicating that ZNF750 plays a reciprocal role in the differentiation of osteoblasts and adipocytes from mesenchymal stem/progenitor cells, thereby contributing to the maintenance of bone homeostasis in mice. Furthermore, we have elucidated the mechanisms that underlie its functional role.

Material and methods

Cell cultures

Mouse BMSCs were isolated from the femurs and tibias following a previously established protocol.[23] Briefly, following the euthanasia of the mice, the femurs and tibias were excised and the marrow was flushed with DMEM. The adherent stromal cells were cultured in a-MEM supplemented with 10% fetal bovine serum (FBS). Additionally, stromal line ST2 cells were maintained in a-MEM with 10% FBS. Cells at passages three to five were induced to differentiate into adipogenic or osteogenic lineages using the appropriate medium at the designated confluence, in accordance with established protocols.[23]

Quantitative RT-PCR

Total RNA was extracted from the cultured cells using a commercially available kit or from tissues utilizing the RNA-easy isolation reagent (Omega). Following this, complementary DNA (cDNA) was synthesized using the RevertAid first-strand cDNA synthesis kit (TransGen Biotech). PCR amplifications were performed in 10 μL reactions containing SYBR Green PCR Master Mix (Zoman Biotech). The primer sequences employed in this study are detailed in Supplementary Table S1. The ΔΔCt method was utilized to assess the expression levels of the target genes, with β-actin serving as the reference gene.

Constructs and transfection

The expression construct of murine Znf750 was obtained from Origene (MR224624). In comparison, the murine Snai1 expression construct was generated by incorporating PCR-amplified CDS region into the pcDNA3.1 vector at BamHI/EcoRI sites using pEASY®-Basic Seamless Cloning and Assembly Kit (TransGen Biotech, Beijing, China). These constructs were utilized for in vitro gain-of-function experiments. In brief, the cells that reached 70% confluence in a 24-well plate were transfected for 4 hours with 0.5 μg of either the Znf750 expression construct or the empty vector, using the Jet PRIME transfection reagent (Polyplus). In contrast, siRNAs were employed for in vitro loss-of-function experiments. The cells were transfected for 24 hours with 16 nM Znf750 siRNAs or negative control siRNA (Generalbiol, Anhui, China) using Lipofectamine RNAiMax (Life Technologies, Gaithersburg, USA). Following transfection, the cells were subjected to adipogenic or osteogenic induction at the appropriate confluence. The sequences of the siRNAs are detailed in Table S2.

Lentiviral packaging and infection

The lentiviral expression construct for Znf750 shRNA was developed by incorporating the annealed oligonucleotide pair that encodes the Znf750 shRNA into the pLVX-shRNA2 vector at BamHI/EcoRI restriction sites. The lentivirus was packaged in 293T cells following a previously described protocol.[24] Primary BMSCs were infected with the lentiviruses at a multiplicity of infection (MOI) of 20. The lentivirus packaged with the empty vector was used as control.

Cell growth assay

Cells were cultured in a 96-well plate. Once reaching 60%-70% confluence, the cells were transfected with the Znf750 expression construct or vector using PEI transfection reagent (MCE) for 8 hours, followed by incubation in refreshed medium for 22 hours. Alternatively, the cells were transfected with Znf750 siRNA or control siRNA using GeticoFect RNAiPlus (Getico Biotech) for 24 hours. Afterward, the cultures were supplemented with 10 μL of CCK-8 solution (Vazyme) per well and subsequently incubated at 37°C for 1 hour. The optical density was then measured at 450 nm.

Western blotting

Cellular proteins were extracted using RIPA lysis buffer, followed by fractionation of 20 μg of proteins via SDS-PAGE and subsequent transfer onto nitrocellulose membranes. The membranes were then blocked with skim milk and probed with primary antibodies at 4°C overnight. This was followed by a 1-hour incubation at room temperature with horseradish peroxidase (HRP)-conjugated secondary antibodies. Protein bands were visualized using a chemiluminescence reagent (ABclonal). The expression levels of each target protein were quantified by calculating the ratio of the grayscale intensity of the respective protein band to that of β-actin. The primary antibodies utilized are detailed in Supplementary Table S3.

Staining of osteoblasts

Transfected cells were cultured in osteogenic medium for 14 days to facilitate differentiation towards osteoblasts followed by ALP staining. After fixation with 4% paraformaldehyde for 15 minutes, the cultures were washed with PBS, and then

incubated with NBT/BCIP staining solution (Beyotime) at room temperature for 15 minutes.

Staining of adipocytes

Transfected cells were cultured in adipogenic medium for 5 days to allow differentiation towards adipocytes followed by oil red O staining. Following a 15-minute fixation with 4% paraformaldehyde, the cultures were rinsed with 60% isopropanol and subsequently incubated in a 0.24% (w/v) oil red O solution for five minutes. To assess the intensity of the staining, the dye was extracted from the cells using 100% isopropanol, and the optical density was measured at a wavelength of 520 nm.

Promoter analysis

The Snail family transcriptional repressor 1 (Snai1) promoter fragment (– 1507/+12 nt) was amplified via PCR from mouse genomic DNA. The resulting fragment was subcloned into the pGL4.14[luc2/Hygro] vector (Promega) at EcoRV/HindIII restriction sites using the pEASY-Basic Seamless Cloning and Assembly Kit. To identify potential ZNF750 binding site "CCTCAGG,"[17] *in silico* analysis was performed using an online tool (https://jaspar.elixir.no/). The identified binding site was subsequently deleted with a site-directed mutagenesis kit (Vazyme).

For the transfection procedure, either the wild-type promoter construct, the mutant promoter construct, or a promoterless vector was co-transfected with the Znf750 expression construct (or pCMV6-Entry vector) into ST2 cells using PEI Transfection Reagent (MCE, Shanghai, China). To assess transfection efficiency, the pRL-SV40 vector was also included. After a 36-hour incubation following transfection, luciferase activity was evaluated using a dual-luciferase reporter assay kit (Yeasen). The relative activity of the promoter was determined by calculating the ratio of firefly luciferase activity to renilla luciferase activity.

Transplantation of primary BMSCs in mice

Primary BMSCs were isolated from C57BL/6J mice aged 4 to 6 weeks and cultured in α-MEM medium supplemented with 10% FBS. At passage 3, the cells were infected with either a lentiviral Znf750 shRNA construct or a control vector for 24 hours.

The sample size of the animal experiment was determined based on a survey of literatures. Fourteen male wild-type C57BL/6J mice, aged eight weeks, were purchased from SPF Biotechnology and housed in the same room in a specific pathogen-free animal facility with controlled temperature and humidity. The mice, 4-5 per cage, had unrestricted access to food and water. After one week acclimatization, the mice were randomly divided into 2 groups: Znf750 shRNA group and control LV group. The BMSCs that expresses either the Znf750 shRNA or the vector were transplanted into the tibial marrow of the respective 2 groups of mice, adhering to a previously established protocol.[25] In brief, under anesthesia, the knee of the mouse was flexed at a 90-degree angle, and a total of 2.5×10^5 BMSCs were injected using a microsyringe filled with Hank's Balanced Salt Solution (HBSS). The syringe needle was inserted through the patellar tendon into the joint surface of the tibia and advanced into the bone marrow cavity. One month after transplantation, the mice were euthanized, and the transplanted tibias were excised for micro-computed tomography (μCT) analysis and histological staining. All animals were included for data analysis.

μCT analyses

The tibias that underwent transplantation were scanned using a Vivo-CT80 μCT scanner (Scanco Medical) with the following parameters: a voxel size of 10.4 μm, an energy setting of 55 kVp, an intensity of 145 μA, a field of view/diameter of 31.9 mm, and an integration time of 300 milliseconds. To assess the architecture and quality of the bone, several metrics were computed, including trabecular bone volume fraction (BV/TV %), trabecular thickness (Tb. Th.), trabecular number (Tb. N.), trabecular bone mineral density (BMD), structural index model (SMI), and cortical thickness (Ct. Th). Three-dimensional reconstructions were generated using the scanner's built-in software. The analysis region for the cancellous bone began 0.1 mm beneath the growth plate and extended over a distance of 1 mm. In contrast, the measurements for the cortical bone began 2 mm beneath the growth plate and extended 0.5 mm further down.

Histological staining

Freshly excised tibias were fixed in 10% formalin for 3 days, followed by decalcification in 14% EDTA (pH 7.4) for 21 days. The samples were then dehydrated through a series of graded ethanol solutions and embedded in paraffin. Sagittal sections were then prepared at a thickness of 4 μm. These sections underwent standard hematoxylin and eosin (H&E) staining, allowing for the quantification of adipocytes and the measurement of their respective areas. Additionally, the sections were subjected to tartrate-resistant acid phosphatase (TRAP) staining, following a previously published procedure.[23] The region of interest for analysis was defined to commence 0.1 mm below the growth plate and to extend over a distance of 1 mm.

Immunohistochemical (IHC) staining

Paraffin sections were baked at 60 °C 2 hours, followed by deparaffinization and rehydration. Antigen retrieval was performed using 0.075% trypsin at 37 °C for 30 minutes. Subsequently, endogenous peroxidase activity was eliminated using 3% hydrogen peroxide, and blocking was achieved with 1% bovine serum albumin (BSA). The sections were then incubated overnight at 4 °C with an anti-ALP antibody (ET1601-21, HuaBio). Following this, the sections were incubated with HRP-conjugated secondary antibody at 37 °C for 1 hour. Staining was developed using 3,3′-diaminobenzidine (DAB) solution, while the nuclei were counterstained with hematoxylin for 3 seconds.

Statistical analysis

Data are expressed as mean ± SD. Differences between 2 groups were assessed using Student's *t*-test with Welch's correction, while comparisons among multiple groups were conducted using analysis of variance (ANOVA). Dunnett's test was performed following one-way ANOVA and Least Significant Difference test was conducted following 2-way ANOVA if ANOVA indicated significant difference. $P < .05$ was considered statistically significant.

Results

Znf750 expression increased during osteogenic differentiation of mesenchymal stem/progenitor cells

The mRNA expression levels of Znf750 were assessed across various normal tissues in 8-week-old mice, indicating

the highest expression in bone, moderate level in liver, and lower levels in other tissues (Supplementary Figure S1A). Additionally, the mRNA expression of Znf750 was tracked during the osteogenic differentiation of ST2 cells and primary cultured BMSCs, demonstrating an increase at intermediate stage (days 3– 9) in ST2 cells and at late stage (days 9–13) in primary BMSCs (Supplementary Figure S1B, C). Notably, a substantial reduction of 92% in Znf750 mRNA expression was noted in the calvarial bone of 18-month-old mice when compared to that of 3-month-old mice (Supplementary Figure S1D).

ZNF750 promoted osteoblast differentiation

The function of ZNF750 in the differentiation of osteoblasts was evaluated through both gain-of-function and loss-of-function experiments. In the gain-of-function study, ZNF750 was overexpressed in ST2 cells via transfection with an overexpression construct (Figure 1A). ZNF750 overexpression did not significantly alter the cell growth rate (Figure 1B). Following osteogenic induction, the overexpression of ZNF750 facilitated osteoblast differentiation, as demonstrated by enhanced alkaline phosphatase (ALP) staining (Figure 1C) and increased mRNA and protein levels of osteogenic markers, including Runx2, osterix, ALP, and osteopontin (Figure 1D, E). Conversely, in the loss-of-function experiments, ZNF750 was downregulated in ST2 cells through transfection with siRNAs (Figure 1F). The depletion of ZNF750 did not significantly alter the cell growth rate (Figure 1G). Under osteogenic induction, the depletion of ZNF750 resulted in a reduction in osteoblast differentiation, as indicated by diminished ALP staining (Figure 1H) and the downregulation of mRNA and protein levels of osteogenic factors (Figure 1I, J).

ZNF750 suppressed adipocyte differentiation

The role of ZNF750 in adipocyte differentiation was evaluated through gain-of-function and loss-of-function experiments. In the gain-of-function study, ZNF750 was overexpressed in C3H10T1/2 cells via transfection with an overexpression construct (Figure 2A). Under adipogenic induction, the overexpression of ZNF750 was found to inhibit adipocyte differentiation, as demonstrated by diminished oil red O staining (Figure 2B, C), and downregulation of mRNA and protein levels of key adipogenic factors, including PPARγ, C/EBPα, fatty acid binding protein 4 (FABP4) and adipsin (Figure 2D, E). In the loss-of-function study, ZNF750 was downregulated in C3H10T1/2 cells through transfection with the siRNAs (Figure 2F). Under adipogenic induction, ZNF750 depletion enhanced adipogenic differentiation, as evidenced by intensified oil red O staining (Figure 2G, H) and upregulation of mRNA and protein levels of adipogenic factors (Figure 2I, J).

ZNF750 transcriptionally downregulated SNAI1 expression and activated Wnt/β-catenin signaling

It has recently been reported that ZNF750 binds to the promoter of Snai1 and depresses its activity in human esophageal squamous cell carcinoma cells.[26] We demonstrated that in murine ST2 cells ZNF750 overexpression resulted in a downregulation of Snai1 mRNA (Figure 3A). Through in silico bioinformatics analysis, we identified a potential binding site for ZNF750 on the proximal promoter of Snai1 located at -658 nt (Figure 3B). To further investigate the functional significance of this binding site, we conducted a luciferase assay with a cloned wild-type promoter construct. The wild-type promoter exhibited transcriptional activity that was diminished upon overexpression of ZNF750. In contrast, the inhibitory effect of ZNF750 on Snai1 promoter was negated when the putative binding site at -658 nt was deleted (Figure 3C).

It is known that SNAI1 acts in concert with Wnt/β-catenin signaling to promote cancer cell invasion and proliferation.[27] Herein we investigated whether ZNF750 and SNAI1 affects Wnt/β-catenin signaling in mesenchymal progenitor cells. The data showed that overexpression of ZNF750 increased phosphorylated protein of glycogen synthase kinase 3β (p-GSK3β) and active non-phospho-β-catenin (non-p-β-catenin), while silencing Znf750 resulted in a decrease in these proteins (Figure 3D, E). Conversely, overexpression of SNAI1 downregulated, while silencing of SNAI1 upregulated these proteins (Figure 3F, G).

To further substantiate the involvement of Wnt/β-catenin signaling in ZNF750-regulated osteogenesis, we performed Znf750 silencing under the background of Wnt/β-catenin activation. The results indicated that the inhibition of osteoblast differentiation, as evidenced by diminished ALP staining and reduced expression of osteogenic factors due to Znf750 siRNA transfection, was mitigated in the presence of CHIR99021, a β-catenin agonist that functions by inhibiting GSK3β activity (Supplementary Figure S2A-C).

SNAI1 exerted opposing effects on osteogenic and adipogenic differentiation in contrast to ZNF750

Subsequently, we investigated the regulatory role of SNAI1 in the differentiation of mesenchymal cell lines. The results showed that the overexpression of SNAI1 suppressed osteogenic differentiation of ST2 cells (Figure 4A-D), whereas the depletion of SNAI1 facilitated this process (Figure 4E-H). In contrast, overexpression of SNAI1 positively regulated the adipogenic differentiation of C3H10T1/2 cells (Supplementary Figure S3A-E), while its depletion restrained adipogenic differentiation (Supplementary Figure S3F-J).

Overexpression of SNAI1 mitigated the dysregulated differentiation of mesenchymal progenitor cells induced by ZNF750

To gain further insight into the potential involvement of SNAI1 in the ZNF750-regulated cell differentiation, a co-transfection experiment was conducted. The findings revealed that the increase of p-GSK3β and non-p-β-catenin levels in ST2 cells due to Znf750 overexpression was attenuated when the Znf750 expression construct was co-transfected with the Snai1 expression construct (Figure 5A). Upon osteogenic induction, ST2 cells co-transfected with the Znf750 expression construct and vector exhibited increased osteogenic differentiation upon osteogenic induction, as evidenced by intensified ALP staining and elevated expression levels of osteogenic factors, in comparison to those co-transfected with vector alone. However, this stimulatory effect was mitigated when the Znf750 expression construct was co-transfected with the Snai1 expression construct (Figure 5B-D). In contrast, when exposed to adipogenic induction, the suppressive effect of Znf750 overexpression on adipogenic differentiation of C3H10T1/2 cells was mitigated when the Znf750 expression construct was co-transfected with the Snai1 expression construct (Figure 5E-H).

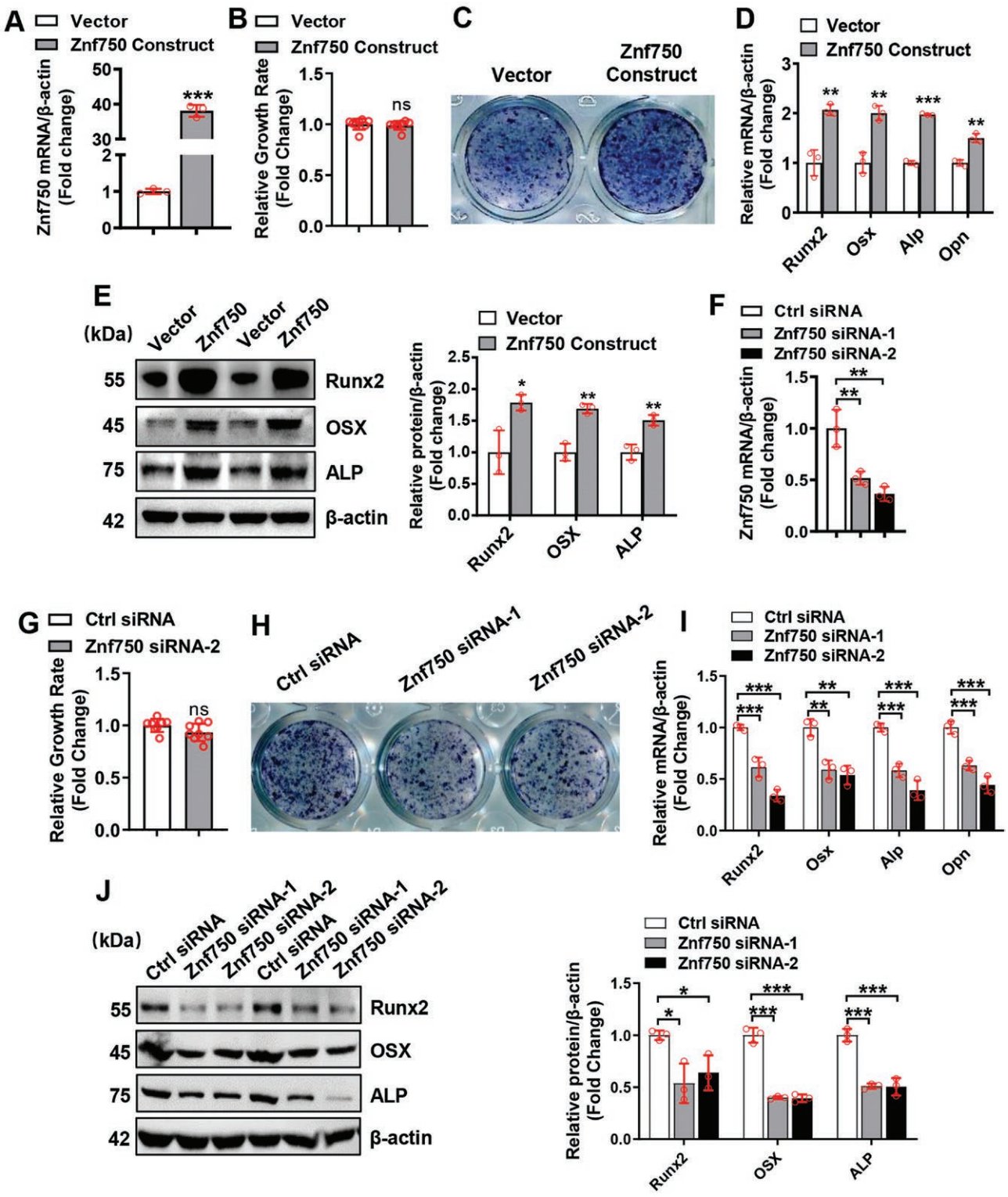

Figure 1. ZNF750 promoted osteoblast differentiation. ST2 cells were transfected with Znf750 expression construct (A) or siRNAs (F). RT-qPCR was employed to measure the mRNA levels of Znf750 in ST2 cells after 48 hours of transfection. The cell growth rate was measured using CCK-8 method (B, G). Transfected cells were induced to allow osteogenic differentiation. ALP staining was performed (C, H). RT-qPCR (D, I) and Western blotting (E, J) were employed to measure the mRNA and protein levels of osteogenic factors after 72 hours of osteogenic induction. Values are mean ± SD, n = 3, *p < 0.05, **p < 0.01, ***p < 0.001 *vs.* vector or control siRNA.

Transplantation of Znf750-silenced BMSCs led to a reduction in cancellous bone mass in mice

In an effort to further elucidate the role of ZNF750 in vivo, we conducted a transplantation study using Znf750-silenced BMSCs, which were generated by infecting BMSCs with a lentivirus expressing Znf750 shRNA. It was observed that depletion of ZNF750 in primary BMSCs inhibited osteogenic differentiation under osteogenic induction (Figure S4A-D),

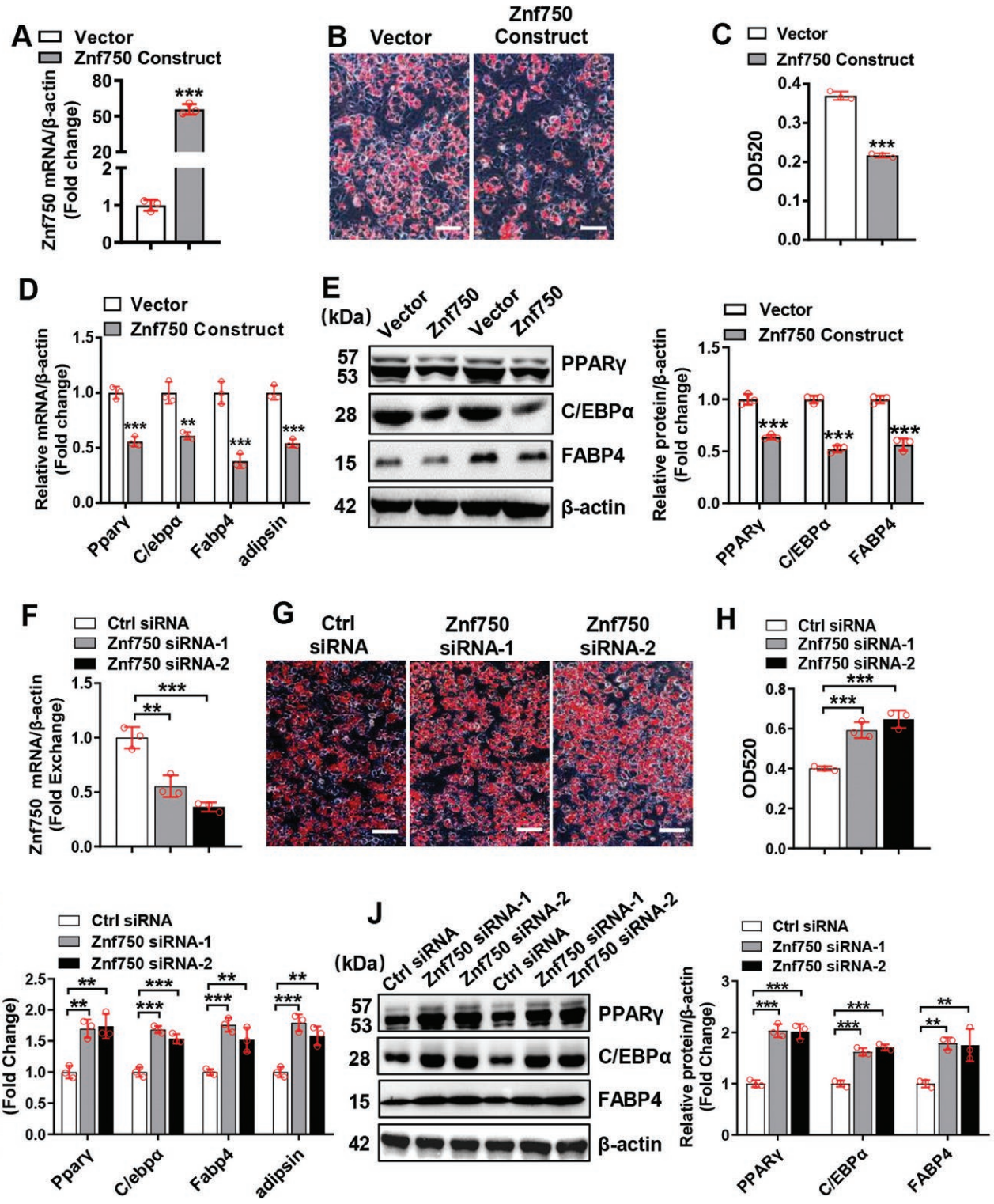

Figure 2. ZNF750 suppressed adipocyte differentiation. C3H10T1/2 cells were transfected with Znf750 expression construct (A) or siRNAs (F). RT-qPCR was employed to measure the mRNA levels of Znf750 in the cells 48 h after transfection. Transfected cells were induced to allow adipogenic differentiation. Oil red O staining was performed after 5 days of adipogenic induction (B, G). The staining intensity was assessed by extracting the stain from the cells and measuring OD520 (C, H). RT-qPCR (D, I) and Western blotting (E, J) were employed to measure the mRNA and protein levels of adipogenic factors after 2 days and 3 days of adipogenic induction, respectively. Scale in (B, G): 100 μm. Values are mean ± SD, n = 3, $^{**}p < 0.01$, $^{***}p < 0.001$ *vs.* vector or control siRNA.

and conversely enhanced adipocyte differentiation under adipogenic induction (Figure S4E-H).

The Znf750-silenced BMSCs were transplanted into the marrow of mice. After a one-month period, the architecture and mass of the transplanted tibias were examined. μCT analysis revealed a significant reduction in trabecular bone volume/total volume (Tb. BV/TV) by 29.3%, trabecular thickness (Tb. Th) by 16.3%, and trabecular bone mineral density (Tb.

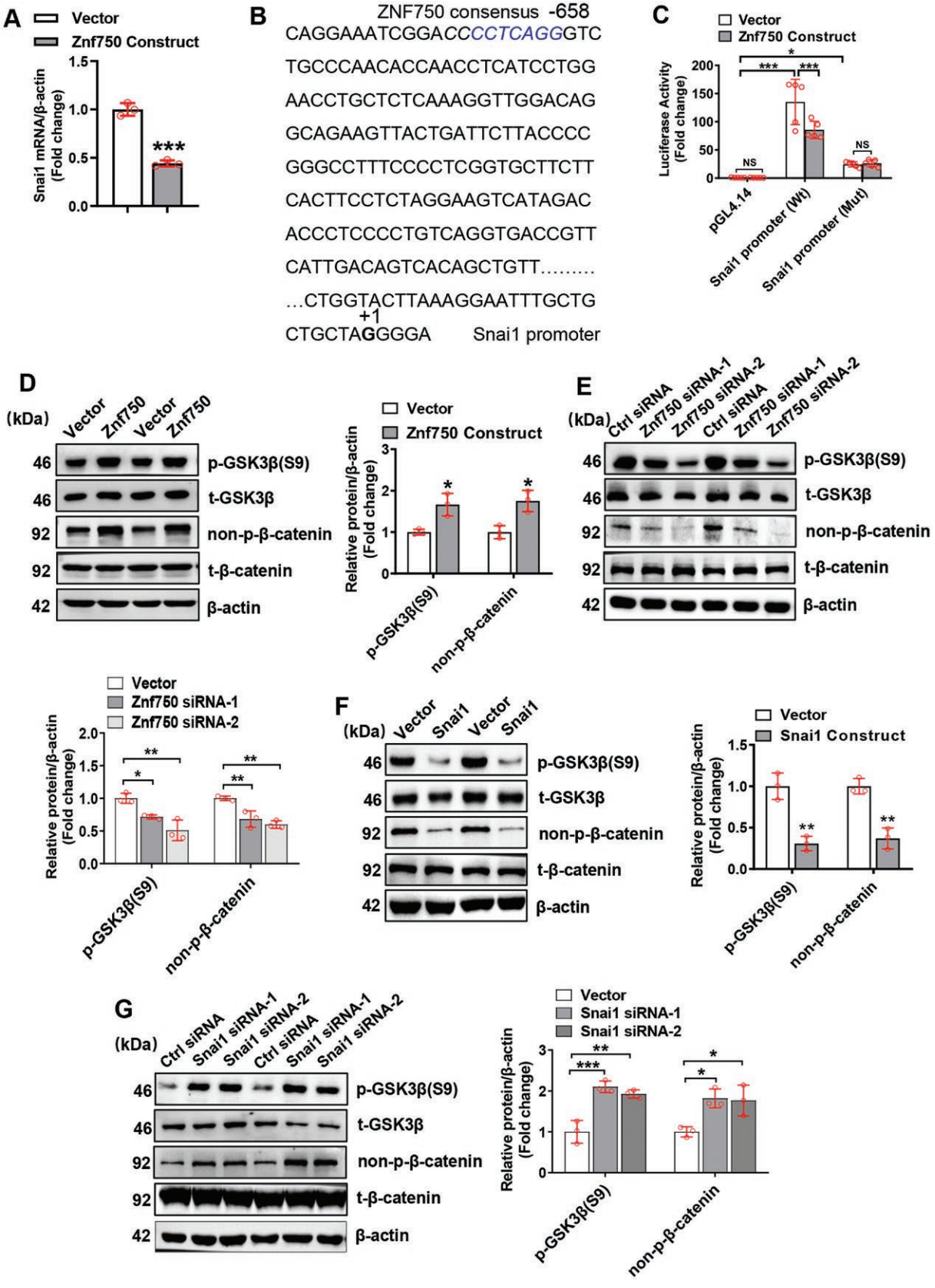

Figure 3. ZNF750 transcriptionally downregulated SNAI1 expression and activated Wnt/β-catenin signaling. ST2 cells were transfected with Znf750 expression construct or vector. RT-qPCR was employed to measure the mRNA levels of Snai1 24 h following transfection (A). The potential binding site for ZNF750 on the proximal promoter of Snai1 gene is illustrated (B). The mutant or wild-type promoter construct of Snai1 (or pGL4.14[luc2/Hygro] vector) was co-transfected with Znf750 expression construct (or vector) into ST2 cells and luciferase activity was measured 48 h after transfection (C). Western blotting was performed to assess the protein levels of p-GSK3β(S9) and non-p-β-catenin in ST2 cells 48 h after transfection with either the Znf750 expression construct (or vector) (D), Znf750 siRNAs (or control siRNA) (E), Snai1 expression construct (or vector) (F), or Snai1 siRNA (or control siRNA) (G). Values are mean ± SD, n = 3. *p < 0.05, **p < 0.01, ***p < 0.001; NS: no significance.

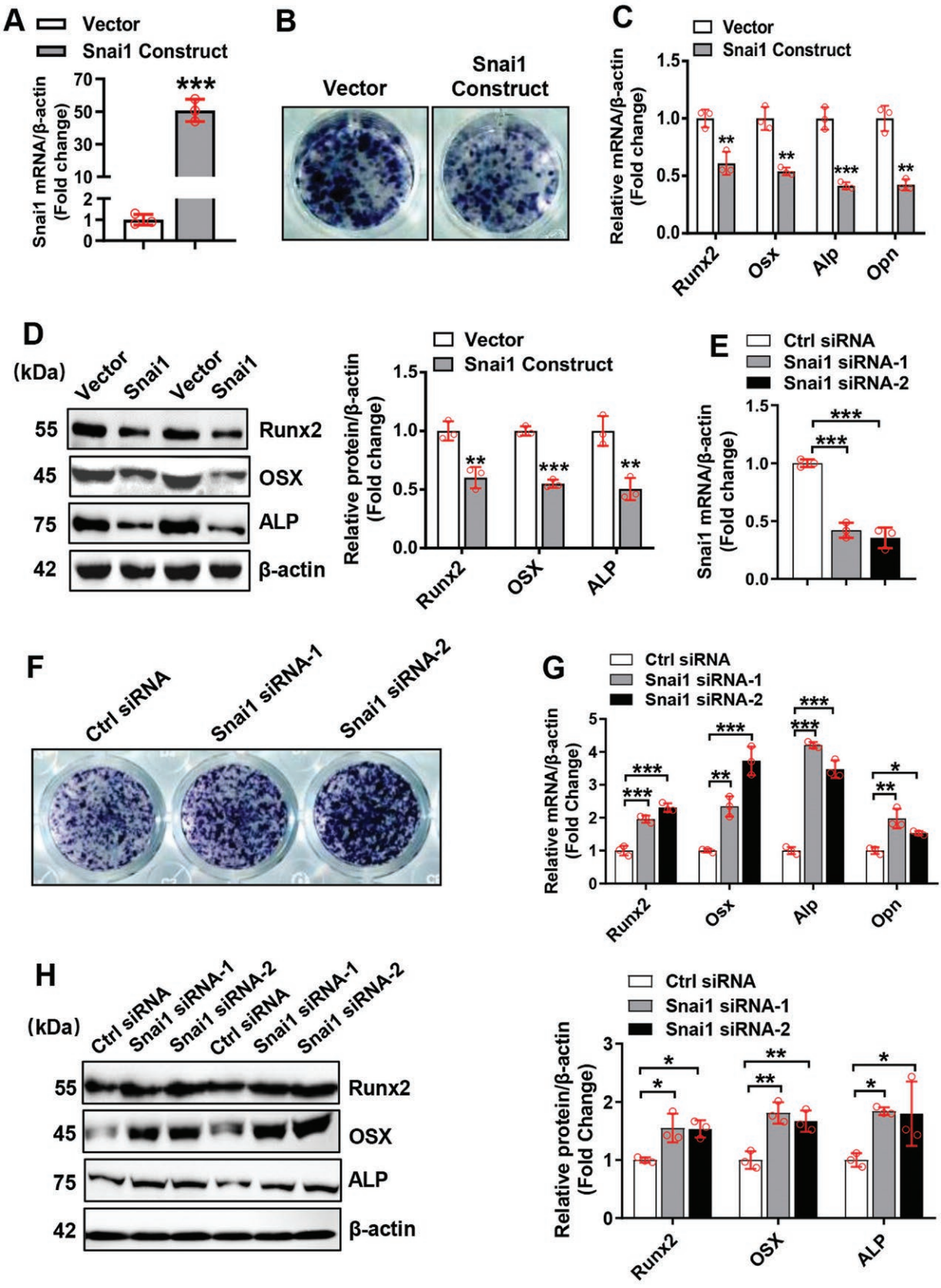

Figure 4. SNAI1 suppressed osteogenic differentiation of mesenchymal progenitor cells. ST2 cells were transfected with Snai1 expression construct (A) or siRNAs (E). RT-qPCR was employed to measure the mRNA levels of Snai1 24 h following transfection. Transfected cells were induced to allow osteogenic differentiation. ALP staining was performed after 14 days of osteogenic induction (B, F). RT-qPCR (C, G) and Western blotting (D, H) were employed to measure the mRNA and protein levels of osteogenic factors following 3 days of osteogenic induction. Values are mean ± SD, n = 3. *p < 0.05, **p < 0.01, ***p < 0.001 *vs.* vector or control siRNA.

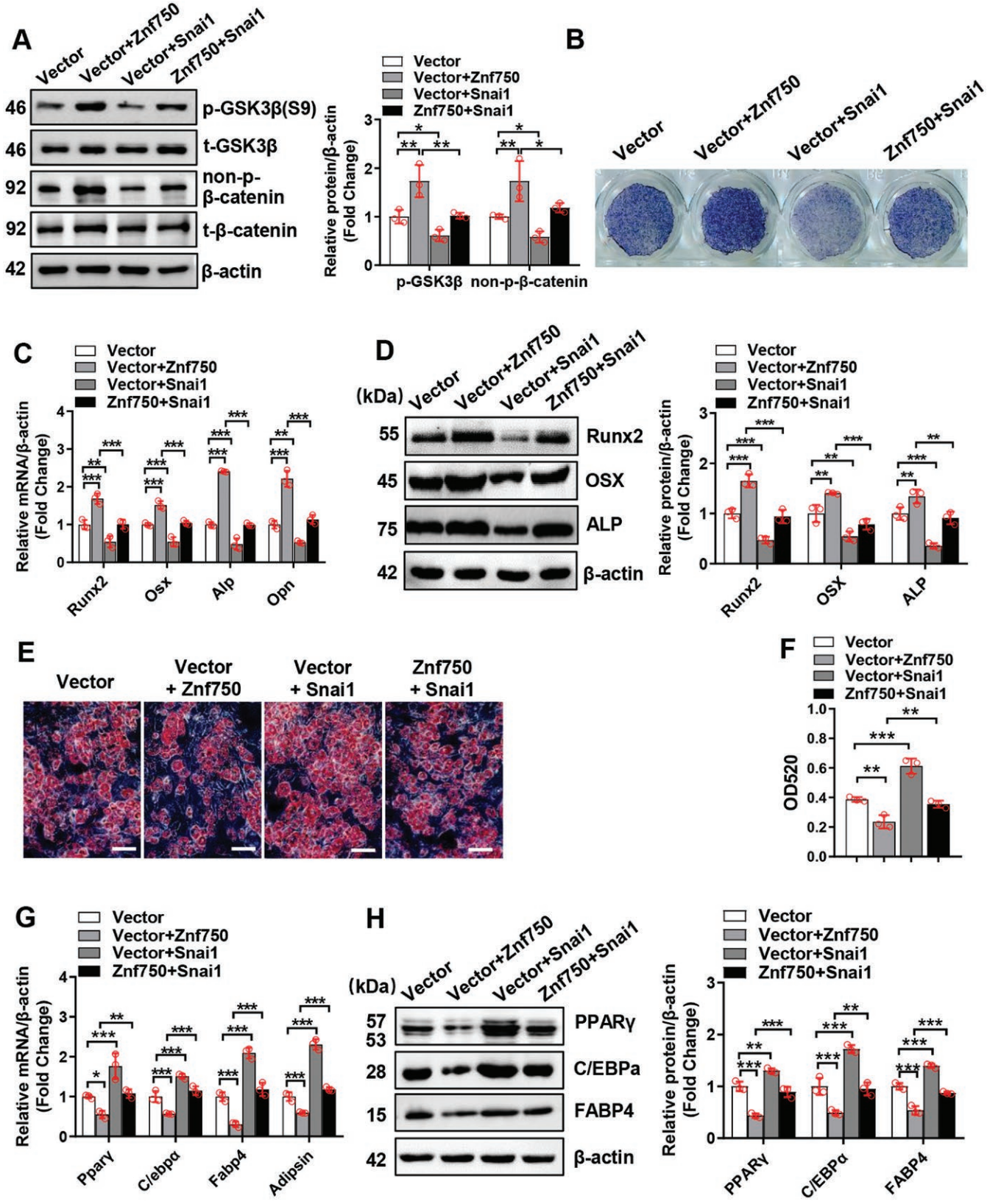

Figure 5. Overexpression of SNAI1 mitigated the dysregulated differentiation of mesenchymal progenitor cells induced by ZNF750. ST2 cells (A-D) and C3H10T1/2 cells (E-H) were co-transfected with Znf750 expression construct (or vector) along with Snai1 expression construct (or vector), respectively. The total and phosphorylated protein levels of GSK3β and β-catenin were assessed using Western blotting (A). Transfected cells were induced to allow osteogenic differentiation (B-D) or adipogenic differentiation (E-H). ALP staining was performed after 14 days of osteogenic induction (B). RT-qPCR (C) and Western blotting (D) were employed to assess the mRNA and protein levels of osteogenic factors after 3 days of osteogenic induction. Oil red O staining was performed after 5 days of adipogenic induction (E). The staining intensity was assessed by measuring OD520 values of the stain extracts (F). RT-qPCR (G) and Western blotting (H) were employed to assess the mRNA and protein levels of adipogenic factors after 2 and 3 days of adipogenic induction, respectively. Scale in (E): 100 μm. Values are mean ± SD, n = 3, *p < 0.05, **p < 0.01, ***p < 0.001 *vs.* vector.

BMD) by 24.8% in mice receiving Znf750-silenced BMSCs compared to those receiving vector-transduced BMSCs. Additionally, the structural model index (SMI) exhibited a notable increase of 23% in the Znf750-silenced BMSC group (Figure 6A-E). In contrast, there was no significant difference observed in trabecular number (Tb. N) between the 2 groups (Figure 6F). Furthermore, cortical thickness (Cort. Th) was decreased by 9% in the Znf750-silenced BMSC group (Figure 6G, H).

Transplantation of Znf750-silenced BMSCs resulted in a decrease in osteoblasts and an increase in adipocytes in mice

To further elucidate the cellular basis for the observed bone phenotype, immunohistochemical staining for osteocalcin revealed a 46% reduction in osteoblasts on the tibial trabeculae of mice transplanted with Znf750-silenced BMSCs compared to those receiving vector-transduced BMSCs (Figure 7A, B). Conversely, H&E staining revealed an increase in both the number (by 2.8-fold) and area percentage (by 5.2-fold) of marrow adipocytes in the mice transplanted with Znf750-silenced BMSCs compared to those transplanted with vector-transduced BMSCs (Figure 7C-E). Additionally, TRAP staining and subsequent osteoclast counting showed no significant differences between the two groups (Figure 7F, G).

Discussion

Although the functions of ZNF750 in epidermal homeostasis and in tumorigenesis have been extensively studied,[19-22] its roles in the development and homeostasis of most tissues have yet to be investigated. Among the various tissues examined, bone exhibits the highest expression level of ZNF750, suggesting its potential involvement in bone homeostasis. Further research revealed a significant rise in ZNF750 expression during osteogenic differentiation, highlighting its potential biological relevance in osteogenesis.

It has been established that ZNF750 inhibits the proliferation of tumor cells.[19,21,28] Furthermore, prior studies have predominantly concentrated on the role of ZNF750 in cell differentiation within epidermal tissue.[15,29,30] In the current investigation, we sought to elucidate the function of ZNF750 in regulating the differentiation of mesenchymal stem/progenitor cells. Through both gain-of-function and loss-of-function experiments, we have demonstrated that ZNF750 promoted osteoblast differentiation while impeding adipocyte

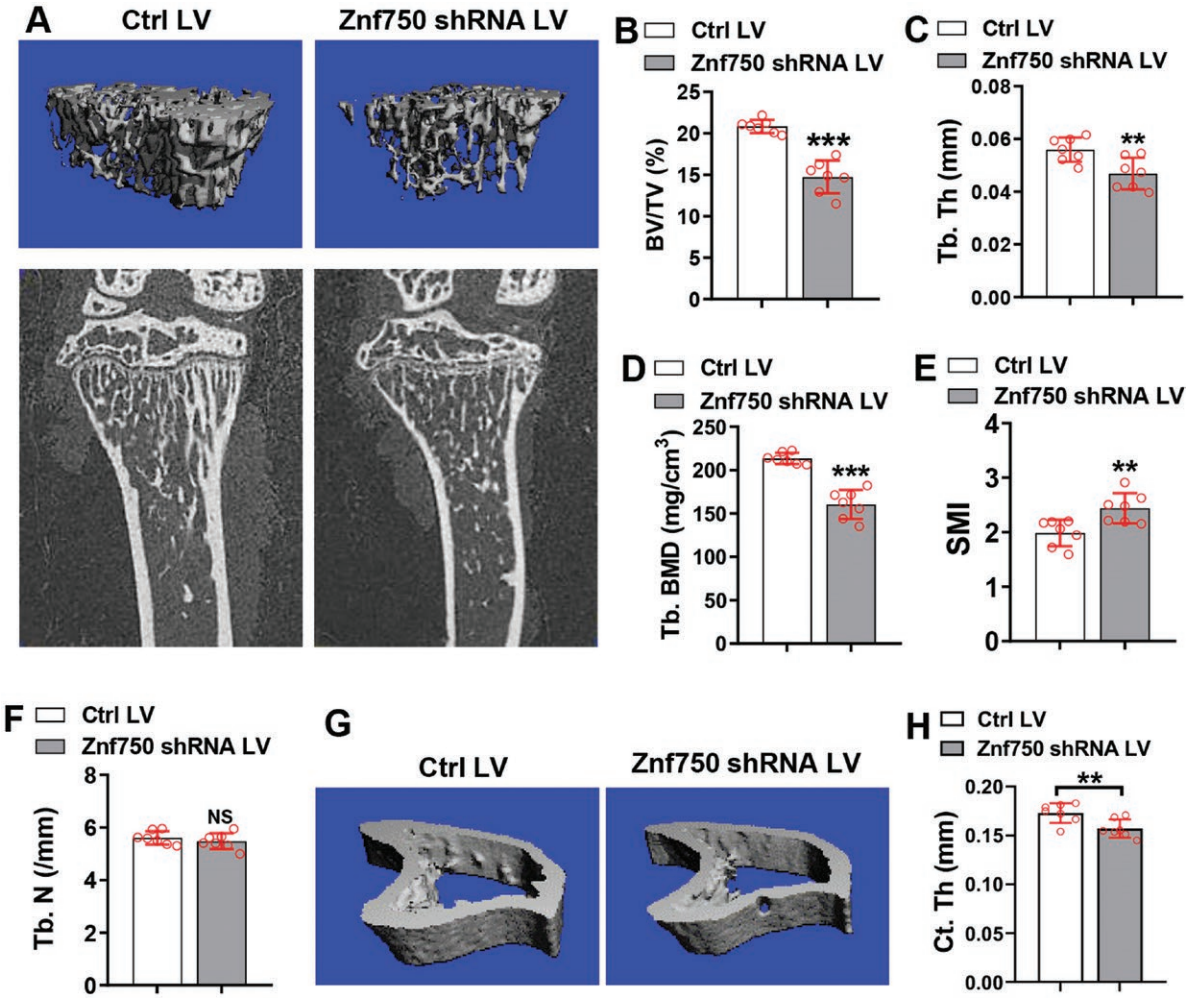

Figure 6. Transplantation of Znf750-silenced BMSCs led to a reduction in cancellous bone mass in mice. Transplanted tibias were scanned by μCT for the analysis of bone mass, and the reconstruction images were generated (A). Histomorphometric parameters were measured and calculated for cancellous bone (B-F) and cortical bone (G, H). Values are mean ± SD, n = 7. *p < 0.05, **p < 0.01, ***p < 0.001, NS: no significance.

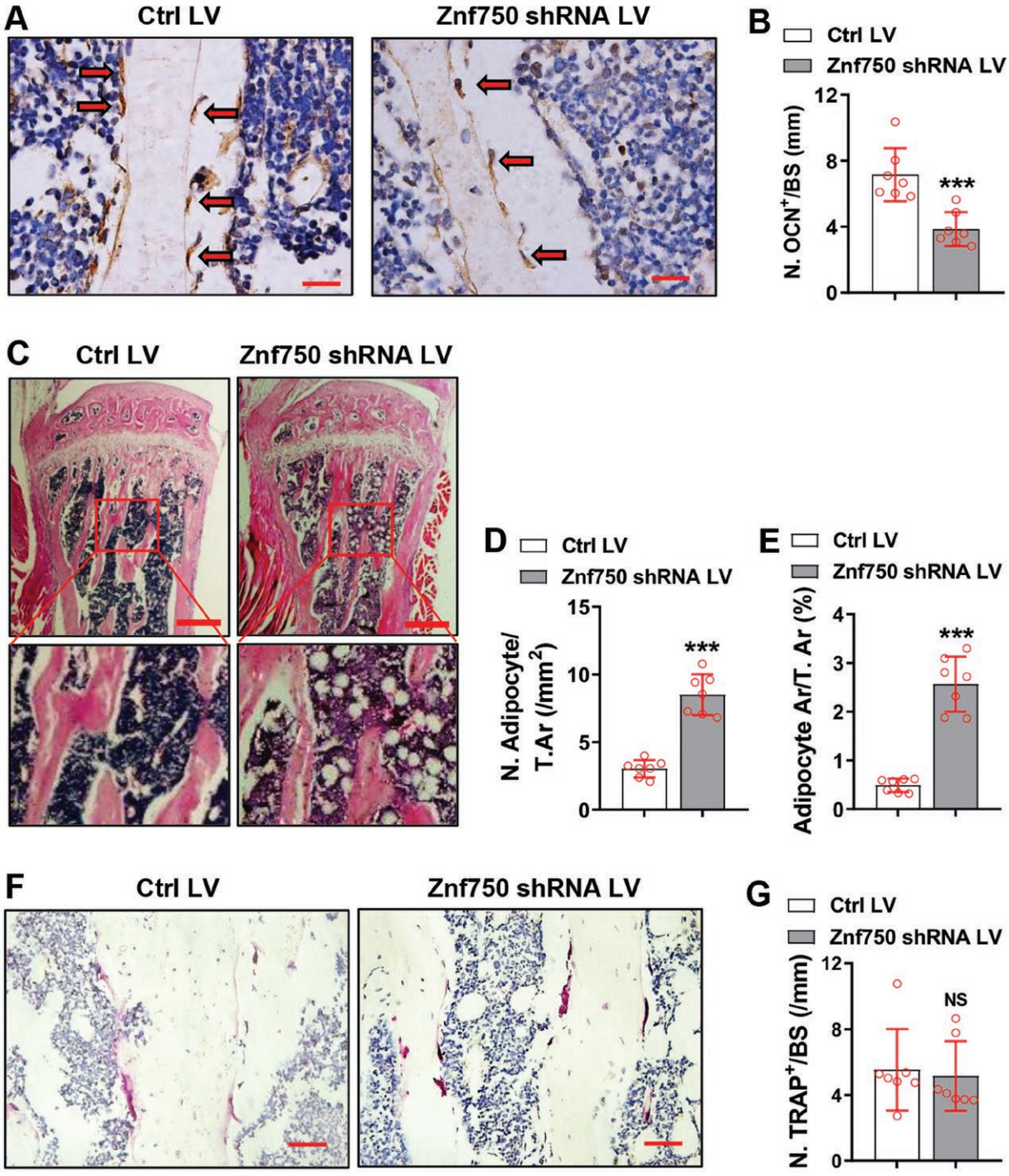

Figure 7. Transplantation of Znf750-silenced BMSCs resulted in a decrease in osteoblasts and an increase in adipocytes in mice. Representative images of osteocalcin IHC staining are shown (A). The numbers of osteoblasts were counted (B). Representative images of H&E staining are shown (C). The numbers of adipocytes were counted (D) and the percentage of area occupied by adipocytes were calculated (E). TRAP staining was performed on the transplanted tibias (F), and the numbers of osteoclasts were quantified (G). Scale bar in (A): 20 μm. Scale bar in (C): 200 μm. Scale bar in (F): 50 μm. Values are mean ± SD, n = 7. ***$p < 0.001$, NS: no significance.

differentiation from primary BMSCs and established mesenchymal progenitor cells.

We further investigated the underlying mechanisms responsible for the regulation of mesenchymal stem/progenitor cell differentiation. Notably, previous studies have indicated that ZNF750 regulates SNAI1 expression in esophageal squamous cell carcinoma cells by binding to the Snai1 gene promoter, thereby impeding the epithelial-mesenchymal transition (EMT) process.[26] Accordingly, we investigated whether ZNF750 transinactivates SNAI1 expression in mesenchymal progenitor cells, and found that ZNF750 downregulated Snai1 mRNA expression. Additionally, ZNF750 suppressed Snai1 promoter activity, with this suppression being contingent upon the putative binding site located at −658 nt.

As a zinc-finger transcription factor, SNAI1 is known to repress the transcription of E-cadherin, thereby influencing

processes such as EMT, embryonic mesoderm formation and maintenance, growth arrest, survival, and cell migration.[31-33] Of note, SNAI1 has been implicated in the modulation of bone mass. Genetic activation of Snai1 in mice hindered osteoblast differentiation by downregulating Runx2 expression.[34] In contrast, specific removal of Snai1 in adipocytes enhanced the expression of adipose triacylglycerol lipase (ATGL) in adipose tissue and promoted lipolysis, leading to a reduction in fat mass and white adipocyte size in mice fed either a standard chow diet or a high-fat diet.[35] In an in vitro research, however, Batlle et al. observed that overexpression of Snai1 in 3T3-L1 pre-adipocytes prevented adipogenic differentiation.[36] In our study, both gain-of-function and loss-of-function experiments revealed that SNAI1 hindered osteoblast differentiation from stromal ST2 cells while it conversely promoted adipocyte differentiation from mesenchymal C3H10T1/2 cells. The discrepancy between our findings and those of Batlle et al. regarding SNAI1's impact on adipocyte differentiation could be due to the use of different cell lines in each study.

In cancer cells SNAI1 acts in concert with canonical Wnt signaling to promote invasion and proliferation.[27] The canonical Wnt signaling pathway facilitates the dedifferentiation of breast cancer cells and augments their invasive behavior through an Axin2-dependent mechanism that stabilizes SNAI1.[37] In return, SNAI1 can trigger the Wnt/β-catenin signaling pathway, thereby facilitating the onset and advancement of colorectal cancer.[38] In the current study, we identified a novel inhibitory effect of SNAI1 on Wnt/β-catenin signaling in mesenchymal progenitor cells, while ZNF750 was shown to activate this pathway. Collectively, the data suggest that ZNF750-mediated activation of Wnt/β-catenin signaling occurs through its transcriptional repression of Snai1 transcription.

We further sought to substantiate the involvement of SNAI1 and Wnt/β-catenin signaling in ZNF750-regulated cell differentiation. The results indicated that the inhibition of osteoblast differentiation caused by Znf750 silencing was mitigated when Wnt/β-catenin signaling was activated. Furthermore, SNAI1 was found to attenuate the activation of Wnt/β-catenin signaling and dysregulated differentiation of osteoblasts and adipocytes triggered by ZNF750. These findings underscore the biological significance of the interaction among ZNF750, SNAI1, and Wnt/β-catenin in the regulation of osteoblast and adipocyte differentiation.

Our subsequent research aims to examine the potential impact of manipulating the Znf750 gene in BMSCs on the balance between osteoblasts and adipocytes, and consequently on bone homeostasis in mice. A single transplantation of BMSCs or adipose-derived stromal cells has been demonstrated to be effective in facilitating osteoblast differentiation, enhancing new bone formation, and improving bone quality.[39,40] As anticipated, the introduction of Znf750-silenced BMSCs into the bone marrow of wild-type mice led to a decrease in both cancellous and cortical bone mass, as evidenced by reductions in the BV/TV and BMD of trabecular bone, as well as cortical bone thickness. Notably, the decrease in cancellous bone volume was primarily attributed to a decrease in trabecular thickness, while the number of trabeculae remained unchanged. Concurrently, there was a decrease in osteoblasts and an increase in marrow adipocytes. Of interest, the increase in adipocytes appears to be more significant than the reduction in osteoblasts. While a definitive conclusion requires additional experiments and a larger sample size to substantiate this observation, the current data may suggest that Znf750 shRNA works more effectively in the adipogenic subpopulation than in the osteogenic subpopulation of BMSCs. These findings indicate that ZNF750 favors osteoblast differentiation while impeding adipocyte formation in vivo, thereby contributing to the maintenance of bone homeostasis.

It is noteworthy that the transplantation of Znf750-silenced BMSCs did not alter the number of osteoclasts in the mice. This observation appears to contradict a previous study which indicated that SNAI1 hindered osteoclast differentiation by suppressing the vitamin D receptor (VDR)-induced RANKL upregulation and OPG downregulation.[34] This discrepancy suggests the presence of other molecules downstream of ZNF750 that may counteract the effect of SNAI1 on the RANKL/OPG ratio, ultimately resulting in a neutral effect of ZNF750 on osteoclastogenesis.

Conclusions

The current study has, for the first time, presented evidence indicating the involvement of ZNF750 in the determination of cell fate in mesenchymal stem/progenitor cells, specifically favoring osteoblast differentiation over adipocyte differentiation. This function is mediated through the SNAI1/β-catenin signaling pathway (Supplementary Figure S5). The reduction of ZNF750 levels in BMSCs leads to a decrease in both cancellous and cortical bone mass in mice, associated with a decline in osteoblasts and an increase in adipocytes in the marrow. ZNF750 may represent a promising therapeutic target for metabolic bone disorders such as osteoporosis.

A limitation of the study is that the in vivo role of ZNF750 is based on the observation of Znf750-silenced BMSCs on bone mass in mice. Further research using a conditional knockout approach is necessary to explore the physiological role of ZNF750 in bone. Additionally, it is crucial to determine the relationship between ZNF750 and bone health in humans.

Acknowledgment

We thank the National Natural Science Foundation of China for funding.

Author contributions

Xiaoli Shi and Xueli Jia (Data curation, Formal Analysis). Wei Liu, Liwen Shi, and Zheng Yang (Data curation). Jie Zhou (Project administration). Xiaoxia Li (Conceptualization, Funding acquisition). Baoli Wang (Conceptualization, Funding acquisition, Writing—original draft). All the authors (Writing—review & editing)

Funding

This work was funded by the National Natural Science Foundation of China (82272444, 82470928), China Postdoctoral Science Foundation (2022M722382), and Tianjin Key Medical Discipline (Specialty) Construction Project (TJWJ2024XK009).

Data availability

All the data that support the findings of this study will be available from the corresponding author upon reasonable request.

Ethics approval and consent to participate

Animal protocols were approved by the Animal Ethics Committee of Tianjin Medical University Chu Hsien-I Memorial Hospital (Approval number: DXBYY-IACUC-2020030; Title: The study on the role and mechanism of transcription factor ZFP750 in regulating the directed differentiation of BMSCs; Approval date: 12/09/2020).

Conflicts of interest

The authors declare no competing interests.

Supplementary material

Supplementary material is available at *Stem Cells Translational Medicine* online.

References

1. Kanis JA. Diagnosis of osteoporosis and assessment of fracture risk. *Lancet*. 2002;359:1929-1936. https://doi.org/10.1016/S0140-6736(02)08761-5
2. Wang J, Liu S, Li J, Zhao S, Yi Z. Roles for miRNAs in osteogenic differentiation of bone marrow mesenchymal stem cells. *Stem Cell Res Ther*. 2019;10:197. https://doi.org/10.1186/s13287-019-1309-7
3. Nehlin JO, Jafari A, Tencerova M, Kassem M. Aging and lineage allocation changes of bone marrow skeletal (stromal) stem cells. *Bone*. 2019;123:265-273. https://doi.org/10.1016/j.bone.2019.03.041
4. Naji A, Eitoku M, Favier B, et al. Biological functions of mesenchymal stem cells and clinical implications. *Cell Mol Life Sci*. 2019;76:3323-3348. https://doi.org/10.1007/s00018-019-03125-1
5. Muruganandan S, Roman AA, Sinal CJ. Adipocyte differentiation of bone marrow-derived mesenchymal stem cells: cross talk with the osteoblastogenic program. *Cell Mol Life Sci*. 2009;66:236-253. https://doi.org/10.1007/s00018-008-8429-z
6. Chen Q, Shou P, Zheng C, et al. Fate decision of mesenchymal stem cells: adipocytes or osteoblasts? *Cell Death Differ*. 2016;23:1128-1139. https://doi.org/10.1038/cdd.2015.168
7. Berendsen AD, Olsen BR. Osteoblast-adipocyte lineage plasticity in tissue development, maintenance and pathology. *Cell Mol Life Sci*. 2014;71:493-497. https://doi.org/10.1007/s00018-013-1440-z
8. Zhong L, Yao L, Tower RJ, et al. Single cell transcriptomics identifies a unique adipose lineage cell population that regulates bone marrow environment. *Elife*. 2020;9:e54695. https://doi.org/10.7554/eLife.54695
9. Baccin C, Al-Sabah J, Velten L, et al. Combined single-cell and spatial transcriptomics reveal the molecular, cellular and spatial bone marrow niche organization. *Nat Cell Biol*. 2020;22:38-48. https://doi.org/10.1038/s41556-019-0439-6
10. Amjadi-Moheb F, Akhavan-Niaki H. Wnt signaling pathway in osteoporosis: Epigenetic regulation, interaction with other signaling pathways, and therapeutic promises. *J Cell Physiol*. 2019;234:14641-14650. https://doi.org/10.1002/jcp.28207
11. Zhang J, Fu M, Cui T, et al. Selective disruption of PPARgamma 2 impairs the development of adipose tissue and insulin sensitivity. *Proc Natl Acad Sci U S A*. 2004;101:10703-10708. https://doi.org/10.1073/pnas.0403652101
12. Wu M, Chen G, Li YP. TGF-beta and BMP signaling in osteoblast, skeletal development, and bone formation, homeostasis and disease. *Bone Res*. 2016;4:16009. https://doi.org/10.1038/boneres.2016.9
13. Nakashima K, Zhou X, Kunkel G, et al. The novel zinc finger-containing transcription factor osterix is required for osteoblast differentiation and bone formation. *Cell*. 2002;108:17-29. https://doi.org/10.1016/s0092-8674(01)00622-5
14. Mevel R, Draper JE, Lie ALM, et al. RUNX transcription factors: orchestrators of development. *Development*. 2019;146:dev148296. https://doi.org/10.1242/dev.148296
15. Sen GL, Boxer LD, Webster DE, et al. ZNF750 is a p63 target gene that induces KLF4 to drive terminal epidermal differentiation. *Dev Cell*. 2012;22:669-677. https://doi.org/10.1016/j.devcel.2011.12.001
16. Birnbaum RY, Zvulunov A, Hallel-Halevy D, et al. Seborrhea-like dermatitis with psoriasiform elements caused by a mutation in ZNF750, encoding a putative C2H2 zinc finger protein. *Nat Genet*. 2006;38:749-751. https://doi.org/10.1038/ng1813
17. Butera A, Agostini M, Cassandri M, et al. ZFP750 affects the cutaneous barrier through regulating lipid metabolism. *Sci Adv*. 2023;9:eadg5423. https://doi.org/10.1126/sciadv.adg5423
18. Schwartz B, Levi H, Menon G, et al. ZNF750 regulates skin barrier function by driving cornified envelope and lipid processing pathways. *J Invest Dermatol*. 2023;144:296-306.e3. https://doi.org/10.1016/j.jid.2023.08.009
19. Zhang P, He Q, Lei Y, et al. m(6)A-mediated ZNF750 repression facilitates nasopharyngeal carcinoma progression. *Cell Death Dis*. 2018;9:1169. https://doi.org/10.1038/s41419-018-1224-3
20. Yang HL, Xu C, Yang YK, et al. ZNF750 exerted its antitumor action in oral squamous cell carcinoma by regulating E2F2. *J Cancer*. 2021;12:7266-7276. https://doi.org/10.7150/jca.63919
21. Ana Choi SS, Ko JM, Yu VZ, Ning L, Lung Maria L. Differentiation-related zinc finger protein 750 suppresses cell growth in esophageal squamous cell carcinoma. *Oncol Lett*. 2021;22:513. https://doi.org/10.3892/ol.2021.12774
22. Butera A, Cassandri M, Rugolo F, Agostini M, Melino G. The ZNF750-RAC1 axis as potential prognostic factor for breast cancer. *Cell Death Discov*. 2020;6:135. https://doi.org/10.1038/s41420-020-00371-2
23. Xie Y, Zhou J, Tian L, et al. miR-196b-5p regulates osteoblast and osteoclast differentiation and bone homeostasis by targeting SEMA3A. *J Bone Miner Res*. 2023;38:1175-1191. https://doi.org/10.1002/jbmr.4834
24. Shi X, Cen Y, Shan L, et al. N-myc downstream regulated gene 1 suppresses osteoblast differentiation through inactivating Wnt/beta-catenin signaling. *Stem Cell Res Ther*. 2022;13:53. https://doi.org/10.1186/s13287-022-02714-5
25. Zhou J, Yang J, Dong Y, et al. Oncostatin M receptor regulates osteoblast differentiation via extracellular signal-regulated kinase/autophagy signaling. *Stem Cell Res Ther*. 2022;13:278. https://doi.org/10.1186/s13287-022-02958-1
26. Kong P, Xu E, Bi Y, et al. Novel ESCC-related gene ZNF750 as potential prognostic biomarker and inhibits epithelial-mesenchymal transition through directly depressing SNAI1 promoter in ESCC. *Theranostics*. 2020;10:1798-1813. https://doi.org/10.7150/thno.38210
27. Freihen V, Ronsch K, Mastroianni J, et al. SNAIL1 employs beta-Catenin-LEF1 complexes to control colorectal cancer cell invasion and proliferation. *Int J Cancer*. 2020;146:2229-2242. https://doi.org/10.1002/ijc.32644
28. Hazawa M, Lin DC, Handral H, et al. ZNF750 is a lineage-specific tumour suppressor in squamous cell carcinoma. *Oncogene*. 2017;36:2243-2254. https://doi.org/10.1038/onc.2016.377
29. Cohen I, Birnbaum RY, Leibson K, et al. ZNF750 is expressed in differentiated keratinocytes and regulates epidermal late differentiation genes. *PLoS One*. 2012;7:e42628. https://doi.org/10.1371/journal.pone.0042628
30. Boxer LD, Barajas B, Tao S, Zhang J, Khavari PA. ZNF750 interacts with KLF4 and RCOR1, KDM1A, and CTBP1/2 chromatin regulators to repress epidermal progenitor genes and induce differentiation genes. *Genes Dev*. 2014;28:2013-2026. https://doi.org/10.1101/gad.246579.114
31. Qi R, Wang J, Jiang Y, et al. Snai1-induced partial epithelial-mesenchymal transition orchestrates p53-p21-mediated G2/M arrest in the progression of renal fibrosis via NF-kappaB-mediated

inflammation. *Cell Death Dis*. 2021;12:44. https://doi.org/10.1038/s41419-020-03322-y
32. Grande MT, Sanchez-Laorden B, Lopez-Blau C, et al. Snail1-induced partial epithelial-to-mesenchymal transition drives renal fibrosis in mice and can be targeted to reverse established disease. *Nat Med*. 2015;21:989-997. https://doi.org/10.1038/nm.3901
33. Carver EA, Jiang R, Lan Y, Oram KF, Gridley T. The mouse snail gene encodes a key regulator of the epithelial-mesenchymal transition. *Mol Cell Biol*. 2001;21:8184-8188. https://doi.org/10.1128/MCB.21.23.8184-8188.2001
34. de Frutos CA, Dacquin R, Vega S, et al. Snail1 controls bone mass by regulating Runx2 and VDR expression during osteoblast differentiation. *EMBO J*. 2009;28:686-696. https://doi.org/10.1038/emboj.2009.23
35. Sun C, Jiang L, Liu Y, et al. Adipose snail1 regulates lipolysis and lipid partitioning by suppressing adipose triacylglycerol lipase expression. *Cell Rep*. 2016;17:2015-2027. https://doi.org/10.1016/j.celrep.2016.10.070
36. Batlle R, Alba-Castellon L, Loubat-Casanovas J, et al. Snail1 controls TGF-beta responsiveness and differentiation of mesenchymal stem cells. *Oncogene*. 2013;32:3381-3389. https://doi.org/10.1038/onc.2012.342
37. Yook JI, Li XY, Ota I, et al. A Wnt-Axin2-GSK3beta cascade regulates Snail1 activity in breast cancer cells. *Nat Cell Biol*. 2006;8:1398-1406. https://doi.org/10.1038/ncb1508
38. Qing F, Xue J, Sui L, et al. Intestinal epithelial SNAI1 promotes the occurrence of colorectal cancer by enhancing EMT and Wnt/beta-catenin signaling. *Med Oncol*. 2023;41:34. https://doi.org/10.1007/s12032-023-02253-w
39. Pauley P, Matthews BG, Wang L, et al. Local transplantation is an effective method for cell delivery in the osteogenesis imperfecta murine model. *Int Orthop*. 2014;38:1955-1962. https://doi.org/10.1007/s00264-013-2249-y
40. Mirsaidi A, Genelin K, Vetsch JR, et al. Therapeutic potential of adipose-derived stromal cells in age-related osteoporosis. *Biomaterials*. 2014;35:7326-7335. https://doi.org/10.1016/j.biomaterials.2014.05.016